Graphene electrodes for electric poling of electro-optic polymer films

Wang, Wen; Wu, Jieyun; Chen, Kaixin; Huang, Quandong; Luo, Jingdong; Chiang, Kin Seng

Published in:
Optics Letters

Published: 15/04/2020

Document Version:
Post-print, also known as Accepted Author Manuscript, Peer-reviewed or Author Final version

Published version (DOI):
10.1364/OL.390656

Publication details:
Wang, W., Wu, J., Chen, K., Huang, Q., Luo, J., & Chiang, K. S. (2020). Graphene electrodes for electric poling of electro-optic polymer films. *Optics Letters*, *45*(8), 2383-2386. Advance online publication. https://doi.org/10.1364/OL.390656

Graphene electrodes for electric poling of electro-optic polymer films

WEN WANG,[1,2,3] JIEYUN WU,[1] KAIXIN CHEN,[1] QUANDONG HUANG,[3] JINGDONG LUO[2,4,*], AND KIN SENG CHIANG[3,*]

[1]*School of Optoelectronic Science and Engineering, University of Electronic Science and Technology of China, No.2006, Xiyuan Ave, West Hi-Tech Zone, Chengdu, China*
[2]*Department of Chemistry, City University of Hong Kong, 83 Tat Chee Avenue, Kowloon, Hong Kong SAR, China*
[3]*Department of Electrical Engineering, City University of Hong Kong, 83 Tat Chee Avenue, Kowloon, Hong Kong SAR, China*
[4]*CityU Shenzhen Research Institute, City University of Hong Kong, No. 8, Yuexing 1st Road, Nanshan District, Shenzhen, China*
**Corresponding author: jingdluo@cityu.edu.hk; eeksc@cityu.edu.hk*

Received XX Month XXXX; revised XX Month, XXXX; accepted XX Month XXXX; posted XX Month XXXX (Doc. ID XXXXX); published XX Month XXXX

We propose electric poling of electro-optic (EO) polymer films with graphene electrodes. The use of graphene electrodes can waive the use of buffer layers and minimize the poling voltage. To demonstrate the idea, we prepared EO polymer thin-film waveguides for poling with traditional Au/ITO electrodes and graphene electrodes, where the EO polymer is a guest-host system formed by doping 15 wt% of dipolar polyene chromophore AJLZ53 into the random copolymer P(S-co-MMA). Our experiments confirm that the use of graphene electrodes can significantly reduce the poling voltage. For a 3.8-μm thick EO polymer film, we achieve high EO coefficients of 82 pm/V at 1541 nm and 110 pm/V at 1300 nm with a poling voltage of 420 V. In addition, the use of graphene electrodes allows more flexible waveguide designs and can potentially simplify the fabrication of devices based on EO polymer.

http://dx.doi.org/10.1364/OL.99.099999

Electro-optic (EO) polymer materials that possess strong, ultrafast EO effects are promising materials for realizing high-performance EO modulators [1–3]. Silicon modulators based on EO polymer that show low driving voltages and large bandwidths have been demonstrated [4–8]. To obtain a large EO coefficient from an EO polymer film, it is necessary to align the chromophores in the EO polymer. This can be done by an electric poling process, where a sufficiently strong electric field is applied across the EO polymer film, while the film is heated up to its glass transition temperature [9]. Traditionally, metal and indium tin oxide (ITO) electrodes are used in electric poling [2–8]. Because the bottom metal electrode cannot be removed after poling, a thick enough buffer layer must be placed between the electrode and the EO polymer film to keep the metal-induced absorption loss low. The presence of the buffer layer, however, increases the poling voltage. The choice of a buffer material that has both high conductivity and good optical transparency is a challenge [4,10]. Sol-gel conductive cladding, whose resistivity is smaller than that of EO polymer by orders of magnitude, is usually used as the buffer material [7,8,11,12], but its synthesis involves complicated chemical processes [11].

In this paper, we propose the use of graphene electrodes for electric poling of EO polymer to exempt the need of using buffer layers and minimize the poling voltage. Our idea is based on the recent finding that a graphene film embedded in or placed on a low-index-contrast waveguide does not induce a significant loss to the transverse-magnetic (TM) waves [13]. This property of graphene has been explored for the realization of a lithium-niobate EO grating [14], a polymer thermo-optic switch [15], and an all-optical switch [16] to improve their performances. In this study, we first calculate the dependence of the graphene-induced loss on the parameters of poled EO polymer. We next prepare two sets of EO polymer films to demonstrate our idea. In one set, which serves as the reference set, the EO polymer film is sandwiched between ITO and gold (Au) electrodes with buffer layers, while in the other set, the EO polymer film is sandwiched between two graphene electrodes without any buffer layers (i.e., the EO polymer film is in direct contact with the graphene electrodes). We compare the poling conditions and the poling results of these samples. Our experiments demonstrate successful electric poling of EO polymer at much lower poling voltages with graphene electrodes. Our results also show that poling with graphene electrodes does not introduce significant additional optical loss to the EO polymer. Another advantage of using graphene electrodes is that the top graphene electrode could be further patterned to form modulation electrodes in the process of fabricating an EO device. The use of graphene electrodes for poling can significantly simplify the fabrication process of EO devices.

Figure 1(a) and 1(b) show the structures of a conventional EO polymer thin-film waveguide with ITO and Au electrodes and our

proposed waveguide with graphene electrodes, respectively. In the conventional structure, the bottom electrode is deposited on the substrate and the cladding of the waveguide serves as a buffer layer to isolate the electrode from the EO polymer film, while the top Au electrode, which is in direct contact with the EO polymer, must be removed after poling. On the other hand, in our proposed structure, the bottom graphene electrode is placed on the cladding and the top graphene electrode is placed on the EO polymer film, i.e., both electrodes are in direct contact with the EO polymer film. As such, the electric field in the EO polymer film generated by the applied voltage depends only on the resistance of the EO polymer film and the poling voltage required is minimized. Most importantly, with the proposed structure, we are free to choose the material and the thickness of the cladding.

In our study, we use EpoClad (Micro Resist Technology GmbH) as the cladding material, which has a refractive index of 1.5595 measured at the wavelength 1537 nm. EpoClad is a durable polymer material with a high glass transition temperature that has been employed to form waveguides embedded in printed circuit boards [17]. We calculate the graphene-induced losses of the TM_0 mode with a commercial mode solver (COMSOL) for different parameters of the EO polymer film, where the monolayer graphene electrodes are modeled as conductive boundaries [13] with a complex conductivity of $6.084 \times 10^{-5} - j7.519 \times 10^{-6}$ at 1550 nm [14] and the material losses of the substrate, the cladding, and the EO polymer are ignored. The refractive index of the EO polymer film after poling depends on the strength of the poling electric field and the EO polymer. The poling process results in an EO coefficient r_{33}, which mainly affects the TM polarization. Before poling, the EO polymer film has an isotropic refractive index. After poling, the EO polymer becomes anisotropic [18]; the refractive index perpendicular to the surface of the waveguide (i.e., along the z direction) increases significantly, while the refractive indices parallel to the waveguide surface (i.e., along the x and y directions) decrease slightly. In our calculation, we vary the refractive index of the EO polymer film along the z direction from 1.58 to 1.68, while fixing the refractive indices along the x and y directions at 1.58.

The results are shown in Fig. 2(a) for the case where only the bottom graphene electrode is present and in Fig. 2(b) for the case that both the bottom and the top graphene electrode are present. A comparison of these two sets of results shows that the top electrode induces a slightly larger loss than the bottom electrode. As shown in Fig. 2, the graphene-induced loss decreases with an increase in the thickness of the EO polymer film, which can be explained by the fact that a stronger light confinement in the EO polymer film with a thicker film leads to a weaker mode field at the graphene electrodes and hence a smaller graphene-induced loss.

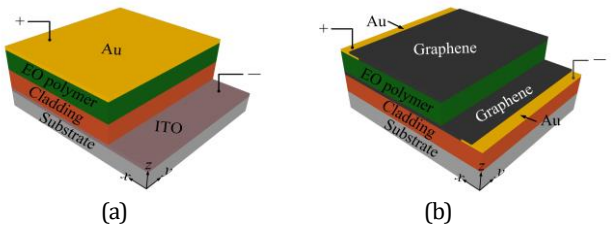

(a) (b)

Fig. 1. Schematic diagrams of EO polymer slab waveguides with (a) conventional Au/ITO electrodes and (b) graphene electrodes, where light propagates in the y direction.

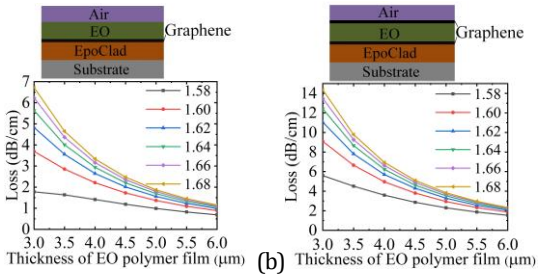

(a) (b)

Fig. 2. Dependence of graphene-induced losses of the TM_0 mode at 1550 nm on the thickness of the EO polymer film calculated at different refractive indices (in the z direction) of the EO polymer for (a) the waveguide with only the bottom graphene electrode and (b) the waveguide with both graphene electrodes.

In general, a large refractive index of the EO polymer leads to a larger graphene-induced loss, which can be explained by the increase in the evanescent field caused by the larger refractive-index contrast. To keep the graphene-induced loss low, we should choose a sufficiently large thickness for the EO polymer film. With a thick enough EO polymer film, the graphene-induced loss becomes insensitive to the refractive index of the EO polymer.

The EO polymer used in this study is a simple guest-host system by doping 15 wt% of dipolar polyene chromophore AJLZ53 into the random copolymer poly(styrene-co-methyl methacrylate) (hereafter AJLZ53/P(S-co-MMA)) [18]. A 6.3 wt% of the solid polymer was dissolved in dibromomethane and filtered with a 0.22-μm polytetrafluoroethylene filter to form an EO polymer solution ready for spin-coating. To fabricate the reference waveguides shown Fig. 1(a), we first spin-coated an EpoClad film on an ITO-coated glass substrate and thermally cured the film. We next spin-coated an EO polymer film onto the cured EpoClad film. To expose the ITO electrode, we scraped some of the polymer film off the substrate. After baking the sample in a vacuum oven at 70 °C overnight, we sputtered a thin layer of Au (~50 nm) onto the EO polymer film as the top electrode. We prepared two reference samples with Au/ITO electrodes: Sample 1, where the thicknesses of the EpoClad and the EO polymer film were 5.1 μm and 4.0 μm, respectively, and Sample 2, where the thicknesses of the EpoClad and the EO polymer film were 4.5 μm and 3.8 μm, respectively. To fabricate the proposed structure shown in Fig. 1(b), we first spin-coated a thick (>10 μm) EpoClad film on a silicon substrate and thermally cured the film. We then sputtered a 5-mm wide Au patch (~50 nm) near the edge of the EpoClad film to facilitate bottom electrode contact. We next wet-transferred a 1.8 x 1 cm^2 graphene/PMMA bilayer (SixCarbon technology, Shenzhen) onto the EpoClad film and removed the PMMA by acetone. The graphene film covered part of the Au patch. We next spin-coated an EO polymer film on the graphene film. Thanks to the large viscosity of the EO polymer, we were able to control the quantity of the EO polymer in the spinning process, so that the Au-connected part of the bottom graphene electrode was left uncoated. We next sputtered a 5-mm wide Au patch (~50 nm) on one side of the EO polymer film to facilitate top electrode contact. We then transferred two separate graphene/PMMA bilayers (with an area of ~1.0 x 1.0 cm^2 each) onto the EO polymer film side-by-side, one of which

covered part of the Au patch. To ensure uniform contact between the graphene films and the EO polymer film, the sample was heated to a temperature near the glass transition temperature of the EO polymer. We kept the thin PMMA layer (~300 nm) in the transfer of the graphene films, as removal of the PMMA layer by acetone would damage the EO polymer film. This thin PMMA layer should not significantly affect the loss of the sample, as confirmed by our simulation. In subsequent experiments, only that part of the EO polymer film covered by the graphene film connected to the Au patch was poled. The other part covered by the graphene film that was not connected to the Au patch was not poled and served as a reference. We prepared two samples with graphene electrodes: Sample 3 and Sample 4, where the thicknesses of the EO polymer film were 3.5 μm and 3.8 μm, respectively.

We poled each sample by applying a voltage ramping up gradually from 0 V to a final voltage with a voltage source (Keithley 2657A), while heating up the sample from 40 °C to 115 °C (the glass transition temperature of the EO polymer) at a rate of 10 °C/min with a hot stage. The resistivity of EO polymer was measured to be in the range of $6 \times 10^8 - 2 \times 10^9$ Ω·m and that of EpoClad was comparable (~10^9 Ω·m). For Sample 1 and 2, the final voltages used were 910 V and 800 V, respectively, and the corresponding electric fields in the EO polymer films were estimated to be ~100 V/μm (assuming the same resistivity for EpoClad and the EO polymer). For Sample 3 and 4, the final voltages used were 350 V and 420 V, respectively, and the corresponding electric fields in the EO polymer films were 100 V/μm and 110 V/μm. The poled areas of Sample 1, 2, 3, and 4 were ~1.2 cm^2, ~0.66 cm^2, ~1.0 cm^2, and ~1.0 cm^2, respectively.

During the poling process, we monitored the leakage current. The rotation of chromophores and polymer chains at the poling voltage and the high temperature gave rise to a rapid increase in the leakage current by more than two orders of magnitude, which is a signature of the completion of the poling process [18]. The variations of the leakage current with the temperature during the poling of the four samples are shown in Fig. 3. The rising of the leakage current reflects the poling characteristics. The leakage currents for Sample 1 and 2 are smaller than those for Sample 3 and 4, which is due to the presence of buffer layers in the first two samples. As the buffer of Sample 1 is thicker than that of Sample 2 (5.1 μm versus 4.5 μm), the poling voltage required for Sample 1 is higher than that of Sample 2. On the other hand, the poling voltages for Sample 3 and 4, which do not contain any buffer layers, are much lower than those for Sample 1 and 2. Furthermore, the leakage current for Sample 4 has the largest value, which indicates that this sample should experience the highest electric-field strength and hence show the best poling result.

After poling, the samples were cooled down to room temperature for further analysis and measurement. For Sample 1

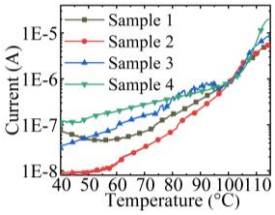

Fig. 3. Variations of the leakage current with the temperature during the poling of the four samples.

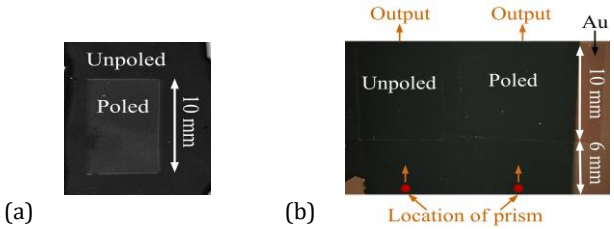

Fig. 4. Photos of poled (a) Sample 2 and (b) Sample 4, showing the poled and unpoled areas on the samples, where in (b) the locations of the prism together with the optical paths for the measurement of the transmission of the TM_0 mode through the poled and unpoled areas, respectively, are highlighted.

and 2, we removed the Au top electrodes with an Au etchant solution. Because the poling process changed the optical absorbance and the refractive index of the EO polymer, the poled and unpoled areas on Sample 1 and 2, which were formed on transparent glass substrates, showed slightly different colors and could be easily differentiated by naked eyes, as shown in Fig. 4(a). On the other hand, visible differentiation of the poled and unpoled areas on Sample 3 and 4 was difficult, as shown in Fig. 4(b), as these samples were formed on opaque silicon substrates.

We measured the refractive indices, the EO coefficients r_{33}, and the propagation losses of the samples with a commercial prism-coupler system (Metricon 2010). Before poling, the refractive indices of the EO polymer films were ~1.58 and ~1.59 for both polarizations at the wavelengths 1541 nm and 1300 nm, respectively. After poling, the refractive indices for the TM polarization were increased significantly, which means that the poled EO polymer films became highly birefringent. We measured the EO coefficients r_{33} of Sample 3 and 4 by directly applying a voltage to each sample and measuring the refractive-index change Δn. The EO coefficient can be estimated from the expression $r_{33} = 2\Delta n/n^3E$, where n is the refractive index of the EO polymer after poling and E is the applied electric field. Because the resistance ratio between EpoClad and the EO polymer was not accurately known, we could not provide an accurate estimate of the r_{33} values for Sample 1 and 2 with this direct measurement method. Nevertheless, by comparing the birefringence values of the EO polymer films of the samples and assuming that the r_{33} value is linearly proportional to the birefringence [18], we could estimate the r_{33} values of Sample 1 and 2.

Table 1 summarizes the refractive indices for the TE and TM polarizations (denoted as n_{TE} and n_{TM}, respectively) and the r_{33} values for the four poled samples at 1300 nm and 1541 nm. In consistency with the poling characteristics shown in Fig. 3, Sample 4 shows the largest r_{33} value, as well as the largest birefringence, while Sample 1 shows the smallest r_{33} value, regardless of the highest poling voltage used. Poled with a lower voltage, Sample 2 exhibits a larger EO effect than Sample 1, which is due to the use of a thinner buffer layer. Sample 3 shows a smaller r_{33} value than Sample 4, because of the use of a lower poling electric field. The highest birefringence values achieved in our work (from Sample 4) are 0.044 at 1541 nm and 0.06 at 1300 nm, and the corresponding r_{33} values are 82 pm/V and 110 pm/V, which are about three times of those of lithium niobate. These values compare well with those

Table 1. Summary of poling results for Sample 1, 2, 3, and 4 (denoted as S1, S2, S3, and S4, respectively)

	Poling Voltage (V)	n_{TE}/n_{TM} at 1300 nm	n_{TE}/n_{TM} at 1541 nm	r_{33} at 1300 nm pm/V	r_{33} at 1541 nm pm/V
S1	910	1.59207/ 1.62082	1.57676/ 1.59824	70	33
S2	800	1.58802/ 1.63826	1.57362/ 1.61040	100	67
S3	350	1.58635/ 1.62818	1.57256/ 1.60368	91	54
S4	420	1.58532/ 1.64593	1.57276/ 1.61682	110	82

reported for similar EO polymer poled with conventional electrodes [18]. Our experiments confirm the feasibility of poling EO polymer at low voltages with graphene electrodes.

We did not observe any visible damages on the EO polymer films after poling. To check whether poling with graphene electrodes might affect the optical loss of the EO polymer, we measured the transmission losses of the TM_0 modes for Sample 3 and 4 using the prism-coupler system [13]. The TM_0 mode guided by the EO polymer film was excited with a collimated laser beam (at 1537 nm) through a high-index prism placed on the area without graphene electrodes. The guided TM_0 mode passed through the area with graphene electrodes and was detected at the end of the waveguide. The transmission was measured for the poled area and the unpoled area, respectively. The locations of the prism and the optical paths for the poled and unpoled areas for Sample 4 are shown in Fig. 4(b) (the layout for Sample 3 is similar). As the optical paths for the probing of the poled and unpoled areas were the same, which, as shown in Fig. 4(b), consist of a 6-mm path without graphene electrodes and a 10-mm path with graphene electrodes, a comparison of the output powers from the two measurements gave the poling-induced loss directly. The poling-induced losses measured in this way for Sample 3 and 4 were ~0.3 dB and ~1.0 dB, respectively. The larger poling-induced loss in Sample 4 could be attributed to the larger birefringence in Sample 4, which, as shown in Fig. 2, should lead to a larger graphene-induced loss.

We also prepared several reference samples, including one that contained only a 3.7-μm thick EO polymer film on a thick EpoClad cladding (i.e., no graphene electrodes), one that contained a waveguide with the bottom graphene electrode, and one that contained a waveguide with both the bottom and the upper graphene electrode. We applied the sliding prism method to these samples and obtained a propagation loss of 2.2 dB/cm for the sample without graphene, 6.2 dB/cm for the sample with the bottom graphene electrode, and 10.6 dB/cm for the sample with both graphene electrodes. The experimental results agree reasonably well with the calculated results, considering the uncertainties in the measurements and the presence of non-uniformity for such large area waveguides. In most practical applications, only a short length of EO polymer film is needed and an upper cladding with a matching refractive index is usually applied, which can reduce the graphene-induced losses. The use of a thicker EO polymer film, as shown in Fig. 2, can significantly reduce the graphene-induced loss. The reason of using relatively thin EO polymer films in our study is to limit the poling voltage required for ITO/Au electrodes and ensure single-mode operation.

In conclusion, we have proposed and demonstrated poling EO polymer films with graphene electrodes. The use of graphene electrodes can do away with buffer layers required for traditional metal electrodes and thus minimize the poling voltage. We have achieved high EO coefficients of 82 pm/V at 1541 nm and 110 pm/V at 1300 nm with a poling voltage of only 420 V, which is much lower than that required by using traditional metal electrodes. The use of graphene electrodes for poling allows the use of inexpensive cladding material and more flexible waveguide designs. The upper graphene electrode can be further patterned to form low-loss modulation electrodes for the EO device to be made. Such a graphene/EO polymer hybrid platform can be explored as a key solution to overcome the traditional tradeoff between poling efficiency and optical loss and significantly simplify the design and fabrication of waveguide devices based on EO polymer.

Funding. Shenzhen Science and Technology Innovation Committee (JCYJ20180507181718203); City University of Hong Kong (CityU) (9610389; 9610452); Science & Technology Department of Sichuan Province (2018JY0092); Fundamental Research Funds for the Central Universities (ZYGX2019Z005); National Postdoctoral Program for Innovative Talents (BX201600027).

Disclosures. The authors declare no conflicts of interest.

REFERENCES

1. J. Wu, B. Wu, W. Wang, K. S. Chiang, A. K.-Y. Jen, and J. Luo, Mater. Chem. Front. **2**, 901 (2018).
2. J. Liu, G Xu, F. Liu, I. Kityk, X. Li, and Z. Zhen, RCS Adv. **5**, 15785 (2015).
3. J. Luo and A. K.-Y. Jen, IEEE J. Sel. Topics Quantum Electron. **19**, 3401012 (2013).
4. D. L. K. Eng, S. T. Kozacik, I. V. Kosilkin, J. P. Wilson, D. D. Ross, S. Shi, L. Dalton, B. C. Olbricht, and D. W. Prather, IEEE J. Sel. Topics Quantum Electron. **19**, 3401306 (2013).
5. X. Zhang, C. Chung, A. Hosseini, H. Subbaraman, J. Luo, A. K-Y. Jen, R. L. Nelson, C. Y-C. Lee, and R. T. Chen, J. Lightw. Technol. **34**, 2941 (2016).
6. L. Alloatti, R. Palmer, S. Diebold., K. P. Pahl, B. Chen, R. Dinu, M. Fournier, J-M. Fedeli, T. Zwick, W. Freude, C. Koos, and J. Leuthold, Light: Sci. Appl. **3**, e173 (2014).
7. H. Sato, H. Miura, F. Qiu, A. M. Spring, T. Kashino, T. Kikuchi, M. Ozawa, H. Nawata, K. Odoi, and S. Yokoyama, Opt. Express **25**,768 (2017).
8. F. Qiu, A. M. Spring, H. Miura, D. Maeda, M. Ozawa, K. Odoi, and S. Yokoyama, ACS Photonics **3**, 780 (2016).
9. L. R. Dalton, P. A. Sullivan, and D. H. Bale, Chem. Rev., **110**, 25 (2010).
10. X. Wang, J. Sun, L. Jin, J. Meng, Y. Yan, C. Chen, F. Wang, and D. Zhang, Mode Phys Lett B. **27**, 1350024 (2013).
11. Y. Enami, C. T. Derose, D. Mathine, C. Loychik, C. Greenlee, R. A. Norwood, T. D. Kim, J. Luo, Y. Tian, A. K.-Y. Jen, and N. Peyghambarian, Nat. Photonics **1**, 180 (2007).
12. S. Huang, T. Kim, J. Luo, S. K. Hau, Z. Shi, X. Zhou, H. Yip, and A. K.-Y. Jen, Appl. Phys. Lett. **96**, 243311 (2010).
13. Z. Chang and K. S. Chiang, Opt. Lett. **41**, 2129 (2016).
14. Z. Chang, W. Jin, and K. S. Chiang, Opt. Lett. **43**, 1718 (2018).
15. X. Wang, W. Jin, Z. Chang, and K. S. Chiang, Opt. Lett. **44**, 1480 (2019).
16. Z. Chang and K. S. Chiang, Opt. Lett. **44**, 3685 (2019).
17. W. Jin, K. S. Chiang, K. P. Lor, H. P. Chan, Jack T. L. To, and R. H. M. Leung, J. Lightw. Technol. **31**, 4045 (2013).
18. J. Luo, D. H. Park, R. Himmelhuber, Z. Zhu, and M. Li, R. A. Norwood, and A. K.-Y. Jen, Opt. Material. Express **7**, 1909 (2017).